ISSN 1330-3651 (Print), ISSN 1848-6339 (Online)
https://doi.org/10.17559/TV-20221204145747
Preliminary communication

Experimental Investigation on the Feasibility and Optimal Frequency of Ultrasonic Assisted Ice Drilling Method

Chen WANG, DaJun ZHAO*, Xin FANG

Abstract: Exploitation of polar resources and scientific research require efficient ice drilling technology. Thermal drilling is a common method for polar ice drilling, and is similar to the principle of ultrasonic assisted drilling; both are drilled by melting ice layers, but improving energy utilization has always been a challenge. In order to improve energy utilization and drilling efficiency, this paper proposes a method for ice drilling with ultrasonic frequency vibration. The mechanism of ultrasonic vibration drilling into ice was analyzed, the solid theoretical foundation for the application of ice melting efficiency under ultrasonic frequency vibration was determined and a series of indoor experiments were conducted. According to experimental data obtained, two conclusions were provided. First, different frequencies have distinct influence on power density, drilling speed and melting rate, and the optimum range excitation frequency for ultrasonic ice drilling is at least 30~32 kHz, under which the ice melting efficiency and drilling speed reached the peak value. Second, ultrasonic assisted drilling was verified to have the ability of improving the efficiency of ice breaking by comparing to thermal drilling under the same power density under 30 kHz. As an environmentally friendly and efficient drilling method, ultrasonic assisted ice drilling has great application prospects in the field of polar exploration. By using Ultrasonic assisted drilling, we demonstrate a strategy for a faster and more efficient drilling method, which is important for humankind.

Keywords: drilling speed; ice drilling; melting efficiency; power density; ultrasound frequency

1 INTRODUCTION

The vast polar region includes glaciers and ice shelves, which are mainly located in Antarctica and Greenland. The glacier stores a large amount of orderly data, with long record sequences, large amount of information, and features of high fidelity and high resolution. Researching on these data is an important method to reveal the earth's climate changing and predict the laws of future environmental changes. Moreover, it is also an effective way to understand historical natural disasters and explore new life forms [1]. This is why researching on polar glaciers is of great economic and humanistic significance. The most important step is to obtain ice cores or sub-ice cores. How to quickly open holes using drilling systems to the core ice layer is the prerequisite for obtaining ice cores effectively. The rate and efficiency of opening holes directly affect the speed and quality of cores. However, the harsh environment conditions in polar regions have forced drilling systems to meet great challenges such as high altitude, low temperature and high wind speed. The lowest temperature in the polar regions can reach –89.5 ℃, and the geological conditions at the bottom of the ice sheets are extremely complex, including snow-packed layers, ice-snow, brittle ice, warm ice layers, ice-rock interlayers, and sub glacial bedrock layers [2, 3]. For these reasons, drilling tools must meet the requirements of low temperature resistance, low energy consumption, light weight and environmental protection.

Thermal drilling method was first proposed in 1963. It is a drilling method that uses resistive elements or thermal fluids to heat the drill bit, melting the bottom ice and achieving ice melt drilling. In the drilling process, the melted water from the melting ice at the bottom flows upward along the outer surface of the bit under the drilling pressure, thus forming a thin film of water between the bit and surrounding ice. The heat generated is continuously transferred to ice layer through this water film, enabling continuous melt water drilling, and a degree of heat loss occurs. As a result, significant energy consumption occurs, and thermal fusion drilling efficiency as well as drilling speed is low. This leads to problems such as hole shrinkage that can easily be triggered during polar drilling open hole work, increasing exploration costs. Furthermore, due to the flow and heat transfer characteristics of the thin film, it is impractical to calculate the energy consumption accurately. This has resulted in empiricism in drilling practice, and a lack of a more unified theoretical guidance yet. The diameter of these drilling bits varies from 18 mm to 150 mm, the power ranges from 0.22 kW to 7.8 kW, and the maximum drilling speed exceeds 20 m/h, while the minimum drilling speed is less than 0.25 m/h [4]. In 2020, academics compared the actual drilling speed of 27 hot melt drill bits with the theoretical drilling speed calculated. The theoretical drilling speed was found to be significantly higher than the actual drilling speed [5].

In view of the above shortcomings of Thermal Drilling method, the concept of ultrasonic assisted drilling provides an attractive option for improving the performance of the rig and enhancing its drilling speed. Ultrasound is a mechanical vibration wave with a frequency of 20 kHz~10^{11} kHz [6]. The reason why choose Ultrasonic Assisted Drilling to speed up drilling efficiency is that ultrasound de-icing technology has been gradually applied to the de-icing of ice-covered high voltage transmission lines, roads and highways and mechanical parts such as paddles and helicopter rotor, it has the characteristics of fast, efficient, convenient operation and is enable to protect the vulnerable environment [7, 8]. In order to verify whether the method is feasible, this paper analyzed the mechanism of ultrasonic ice drilling, established a mathematical calculation, and designed experiments to verify whether the method could be applied to large-scale practice. It will have a significant and far-reaching impact on conducting in-depth exploration of polar regions and the future study of global climate issues.

2 ULTRASONIC DRILLING MECHANISM ANALYSIS AND COMPUTATIONAL MODELING

Ice is low in density and has a low strength open structure with low melting point. Based on its deicing principle, ultrasonic ice drilling mechanism includes thermal mechanism and non-thermal mechanism; the latter can be divided into mechanical mechanism and cavitation

mechanism. These are the theoretical bases to analyze the law of action that changes with the frequency.

2.1 Thermal Mechanism of Ultrasonic Drilling

The thermal mechanism has an ice-melting effect, and the heat generated accelerates the melting of ice. Using the ultrasonic welding principle as a theoretical basis, it is known that the source of heat mainly includes energy storage conversion heat, high-frequency vibration friction heat and cavitation effect accompanying heat [9, 10].

1) Physical vibrational deicing

Theoretically, based on the pressure-strain energy storage mechanism of medium, the high-frequency stretching and squeezing of the ultrasonic drill bit causes the vibration of the ice mass, generating physical vibrational elastic energy and deforming the ice crystal structure [11]. This deformation energy is subsequently converted into endothermic energy of water molecules. The energy transformation and accumulation in drilling process leads to the increase of lattice energy between water molecules, resulting with a degree of thermal motion disorder in the system gradually increasing [12, 13]. With the force of water molecules destroyed, the orderly arrangement of water molecules inside the ice is gradually disordered, as well as the temperature of solid ice rises and thus melts into liquid water. At the same time, the high-frequency vibration of the ultrasonic drill bit effectively agitates the liquid in the bore hole and increases its flow rate when the mass transfer power of water molecules from the ice crystal surface to the fluid increases occurs, destroying the heat transfer boundary and enhancing the heat transfer between liquid water and the ice layer of pore wall [14].

2) Frictional heat generation

The surface of the ultrasonic drill bit has a certain roughness. In the process of vibration, the bit contacts and rubs with the surrounding ice layer, and contact friction occurs. The heat energy generated by this friction process is absorbed by surrounding ice, which destroys the hydrogen bond and reduces the connecting force in water molecules [15]. Under the condition of constant amplitude, the internal frictional motion of the ice mass is strengthened when frequency increases, leading the mass transfer rate to increase and the conversion rate of endothermic energy to accelerate. Among a certain frequency range, thermal effect and the rate of destruction are enhanced with the increase of frequency.

However, if vibration frequency is beyond this range, the excessive friction rate makes the roughness of the surrounding ice decrease. In this situation, the frictional force between the ice and the drill bit decreases, thereby reducing the frictional heat energy, resulting in a decrease in the melting rate, and weakening the effect of the thermal mechanism. Therefore, in order to make the thermal effect reach the optimum, it is important to explore the appropriate ultrasonic vibration frequency range.

3) Ultrasonic-enhanced heat transfer

When the drill starts working, the high-frequency vibration of the bit effectively stirs the fluid in the borehole, increasing the flow rate of the fluid. The mass transfer power of water molecules migrates from the surface between ice crystal and fluid, and the heat transfer boundary is destroyed. As a result, the heat transfer rate between the water and the ice [16]. As the output frequency of the drill bit increases, the intensity of fluid disturbance becomes larger, and the detachment rate of the ice layer is subsequently enhanced, reinforcing the effect of the thermal mechanism.

2.2 Non-Thermal Mechanism of Ultrasonic Drilling

1) Fatigue failure

When ultrasonic mechanical shock is applied on the ice surface, the ice layer is subjected to this continuous steady-state forced vibration excitation, and the response is generated in a limited area and depth. The amplitude of the ice layer changes and gradually reaches to the maximum. Inside ice layers there are series of kinds of micro-defects, such as inside-bubbles and micro-cracks. Under the excitation of ultrasonic vibration, these structures gradually expand and penetrate, increasing in number and size, and undergoing irreversible evolution. This micro-behavioral evolution leads to a decrease in the strength of the ice layer until it reaches the fatigue damage limit, and a macroscopic deformation and large-scale of fragmentation occurs finally.

The whole process of the above amplitude-frequency relationship is divided into three stages [17, 18]. When the excitation frequency is below the ice inherent frequency, the ice response is in the static deformation process, and it is in reversible deformation. When the excitation frequency is higher than the ice inherent frequency, the ice cannot catch up with the high frequency vibration rate of the drill due to inertia, and the ice is only broken in a small area. When the excitation frequency is close to the intrinsic frequency of the ice, the ultrasonic vibration system forms resonance with the ice in a certain range of area and depth. At this time, the ice is under a resonance state, and the response displacement amplitude, steady-state response speed and acceleration of the ice will reach the maximum. The ice layer is easy to occur in a large area effectively broken.

2) Cavitation effect

The ultrasonic cavitation mechanism is brought into effect when a liquid environment is formed in the borehole under the action of the thermal mechanism. There are many tiny vesicular nuclei in the liquid medium, which undergoes a series of kinetic processes of oscillation, growth, contraction and collapse under the action of periodic positive and negative ultrasonic pressure waves triggered by the ultrasonic vibration. As a result, the cavitation effect assists in ice sheet breakup process [19]. The detailed process is described below. When the ultrasound is in the negative pressure phase and reaches a certain intensity, the original integrity of the liquid structure is destroyed. Holes and cavities begin to appear in the liquid and gradually increase in size to form cavitations bubbles [20]. The tension on bubble surface causes the internal air pressure increasing and accumulating until it reaches the bubble tolerance limit. Then these bubbles rupture, and the energy is released instantaneously, producing a transient high temperature (> 5000 K) and high pressure (> 500 GPa) effect [21]. The output ultrasonic frequency magnitude is related to the rapidity of the positive and negative change cycles of the acoustic pressure. It has a direct relationship with the violent and complex motion process of the bubbles. With the increase of ultrasonic excitation frequency, the

cavitation bubble closure phase becomes increasingly faster, then cavitation bubbles burst [22]. At the same time, the strong shock wave and jet effect make the ice crystal nuclei within the borehole ice layer splitting into many discrete tiny ice crystals, which strengthens the effect of the thermal effect [23]. In addition, due to the high velocity gradient and viscous stress on the surface of the vibrating bubble, the growth and fragmentation of the cavitation bubbles cause fluid circulation, resulting in fluid perturbation and accelerating the erosion and stripping of the surrounding ice [24]. Thus, the cavitation effect, as a non-thermal mechanism, acts in conjunction with the thermal effect to assist in the breakup of the ice and further increases the ice drilling rate.

In summary, the optimal frequency exists for ultrasonic ice drilling due to the melting effect of thermal effect and the fatigue damage mechanism of mechanical effect. Therefore, the ultrasonic excitation frequency is used in this article as a variable to explore the law of the effect of above factors on ice drilling.

2.3 Theoretical Formulation of Ultrasonic Drilling Mechanism and Effects

Numerical model ultrasonic deicing effects

According to the above analysis of the ultrasonic ice drilling mechanism, it is clear that under the static pressure condition without rotary cutting, the ultrasonic drill bit drills in the way of melting ice. Therefore, the theoretical study of drilling rate is established with the average power density, drilling speed and ice melting efficiency as the analytical benchmark.

1) Average power density

Physics refers to the work done by an object under a combined external force as total work, which is defined as the work done per unit time as power. Power is a physical quantity that represents the speed at which an object does work. The sum of instantaneous power within a certain time range is the total amount of work done during this time period. According to the principle of calculus, the total input electrical energy and average input power of the ultrasonic transducer during the operating time period T are calculated as follows. Eq. (2) is derived from Eq. (1).

$$W = \int_0^T P_t \mathrm{d}t \tag{1}$$

$$\overline{P} = \frac{W}{T} = \frac{1}{T}\int_0^T P_t \mathrm{d}t \tag{2}$$

W is the total input electrical energy of the ultrasonic vibration system (J), calculated by integrating the power displayed by the drive power supply in real time against the working time T. $\overline{P}$ is the average input electrical power of the ultrasonic vibration system (w). P_t is the instantaneous power of the ultrasonic vibration system (w). T is the working time (s).

Average power density is the input power of ultrasonic vibration system per unit area, which indicates the efficiency of the input energy of the vibration system. It is the ratio of the average input power to the cross-sectional area of the borehole during the drilling time. Eq. (3) can be obtained from Eq. (2).

$$I = \frac{\overline{P}}{A} = \frac{400\int_0^T P_t \mathrm{d}t}{\pi T d^2} \tag{3}$$

where I is average power density (w·cm^{-2}), A is borehole cross-sectional area (cm^2) and d is borehole diameter (mm).

2) Drilling speed

Drilling speed is the ratio of drilling depth to drilling time, as shown in Eq. (4).

$$V = \frac{3.6h}{T} \tag{4}$$

where V is drilling speed (m·h^{-1}).

3) Ice melting efficiency

When drilling completes, the difference in mass before and after drilling of the ice sample needs to be calculated. At this point, the borehole is cylindrical in shape. The formula for calculating the volume of a cylinder is shown in Eq. (5). Therefore, the melting mass of ice sample is the product of the volume of the borehole and the density of the ice at that temperature, as shown in Eq. (6).

$$V = Sh = \pi\left(\frac{d}{2}\right)^2 h = \frac{\pi d^2}{4}h \tag{5}$$

$$\Delta m = \rho V = \rho h \frac{\pi d^2}{4} \times 10^{-3} \tag{6}$$

where Δm is the melting mass of ice sample (g), ρ is the density of ice at that temperature (0.917 g·cm^{-3}), h is the drilling depth (mm), and S is the the cross-sectional area of the borehole (mm).

Let the heat absorbed by the ice phase change process be Q_c and the heat absorbed by the non-phase change process be Q_l during the working time T [25-27]. Substitute into Eq. (6) to obtain Eq. (7) and Eq. (8).

$$Q_c = \Delta m \times C \times \Delta T = \rho h \frac{\pi d^2}{4} \times C \times \Delta T \times 10^{-6} \tag{7}$$

$$Q_l = \Delta m \times L = \rho h \frac{\pi d^2}{4} \times L \times 10^{-6} \tag{8}$$

where Q_c and Q_l are the heat absorbed by ice warming to the melting point and ice melting to water at the same temperature (J), respectively. ΔT is the temperature difference before and after ice melting, which is the difference value between the melting temperature of ice 273.15 K (i.e., 0 °C) and the temperature of frozen ice sample 258.15K (i.e. –15 °C). C is the specific heat capacity of ice (i.e., 2100 J·kg^{-1}K^{-1}) and L is the latent heat of liquefaction of ice (3.36×10^5 J·kg^{-1}).

The sum of Q_c and Q_l is the minimum heat required for ice melt drilling, expressed as effective work Q, as shown in Eq. (9).

$$\begin{aligned} Q &= Q_c + Q_l = \Delta m\left(C \times \Delta T + L\right) = \\ &= \rho h \frac{\pi d^2}{4}\left(C \times \Delta T + L\right) \times 10^{-6} \end{aligned} \tag{9}$$

Based on the above derivation (9), the formula for calculating the efficiency of ultrasonic drilling for ice melting is derived as Eq. (10).

$$\eta = \frac{Q}{W} = \frac{\Delta m\left(C \times \Delta T + L\right)}{4\int_0^T P_t \mathrm{d}t} = \\ = \frac{\rho h \pi d^2 \left(C \times \Delta T + L\right) \times 10^{-6}}{4\int_0^T P_t \mathrm{d}t} \tag{10}$$

3 EXPERIMENTAL MATERIALS AND PROCEDURES

3.1 Testing Equipment

The tests were completed with four sets of intelligent piezoelectric ceramic ultrasonic vibration generators. The main components are the driving power supply, electrical energy piezoelectric ceramic transducer, amplitude rod and tool head (as shown in Fig. 1).

Figure 1 The piezoelectric ceramic ultrasonic vibration generator

These generators can make real-time response to its own frequency according to the change of ultrasonic vibration system parameters, and the generated frequency automatically tracks and matches the resonant frequency of the transducer vibration system to ensure that the system is always in the best resonance state and obtains the maximum amplitude. The working process of ultrasonic generator is as follows. First, the driving power supply converts the 220 V, 50 Hz AC signal into an ultrasonic frequency electrical oscillation signal and is subsequently converted into mechanical vibration by the transducer. Then the variable amplitude rod amplifies the mechanical amplitude, displacement and velocity to gather energy to reduce the loss of ultrasonic energy wave from transmission to the load. Finally, the tool head connected with the rod contacts with the sample directly with its bottom side.

Instrument model and parameters are shown in Tab. 1.

Table 1 Main parameters of ultrasonic vibration generators

Frequency / kHz	Gravity of drill bit / N	Diameter of tool head / mm
20	53.9	26.88
30	24.5	27.00
35	24.5	26.58
40	24.5	26.90

From the data shown above, the weight of drill bit and length of tool head with different frequencies are distinct. In order to control the variables and make the experimental conditions consistent, the bits need to add bob-weight to make the loading weight on bit consistent. Therefore, a pressure plate with a gravity of 29.4 N was placed on the ultrasonic transducer of 30, 35 and 40 kHz, keeping the pressure applied to the ice sample equal to the gravity of the ultrasonic wave at 20 kHz (i.e., 53.9 N).

3.2 Ice Sample Preparation

Ice samples were frozen in test chamber. The internal temperature was set at –15 °C. Then researchers filled the round table-shaped mold with degassed pure water and placed them in the test chamber, together with the ultrasonic vibrator. The mold was taken out after 24 hours, and the upper and lower surfaces were polished and tested with a level to ensure the stability of the tool head during the test. The diameters of the top and bottom surface of the sample after grinding were 40 mm and 60 mm respectively, and the height was 80 mm. The temperature of both the ice sample and the ultrasonic oscillator surface is –15 °C, which could minimize the error caused by heat loss. Parameters of samples are shown in Tab. 2.

Table 2 Parameters of samples

Parameters	Unit	Value
Sample temperature	°C	–15
Top diameter of sample	mm	52
Bottom diameter of sample	mm	70
Sample height	mm	70
Compressive strength	MPa	3

3.3 Experimental Procedure

The main steps of the experiment were as follows.

1) Firstly, place the ice sample smoothly under the drill bit.

2) Secondly, press the tool head on the surface of the ice sample smoothly.

3) Thirdly, press the power switch while start timing, until the tool head was completely plunged into the sample (Fig. 2). Record the input power and operating time. Then turn off the power and stop drilling.

4) Measured the borehole diameter and depth of the ice sample and recorded.

Parallel tests were performed at each frequency and six sets of valid data were obtained, for a total of 40 sets of valid data. Noticeably, the whole process was carried out in the chamber.

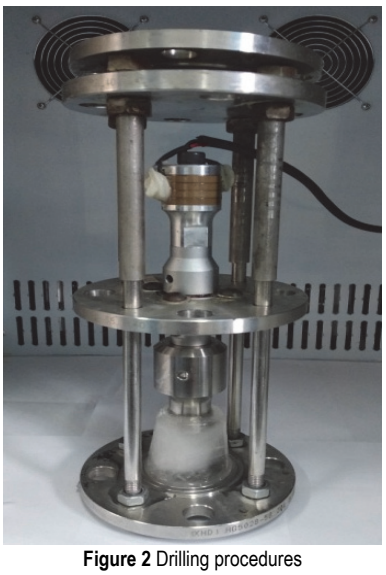

Figure 2 Drilling procedures

4 RESULTS AND DISCUSSION

During the experiment, it was observed that no cracks were visible to the naked eye within the ice, and the tool head dropped steadily in the ice, and liquid water was flowing out of the borehole. After drilling, the ice sample formed regular circular holes, and its diameters were similar to the borehole. The above experimental phenomena indicated that ultrasonic vibration is not dominated by mechanical fatigue crushing drilling, but by melting under the effect of cavitation and thermal effect. Therefore, drawing on the evaluation method of hot-melt drilling tools, it was feasible to evaluate the drilling effect by taking the average power density as the independent variable while taking the melting ice efficiency and drilling speed as the dependent variable indicators.

Based on the deduction of the formulas above, the experimental data under different ultrasonic frequency excitation were calculated separately, and then averaged as shown in Tab. 3. In particular, the input power and operating time of the ultrasonic generator were shown and recorded by the display.

Table 3 Average results under different frequencies

Ultrasonic frequency	Power Density	Drilling speed	Ice melting efficiency
20 kHz	38.90 w·cm^{-2}	1.98 m·h^{-1}	47.7%
30 kHz	25.85w·cm^{-2}	2.29 m·h^{-1}	83.0%
35 kHz	22.53 w·cm^{-2}	1.76 m·h^{-1}	73.3%
40 kHz	16.01 w·cm^{-2}	1.18 m·h^{-1}	69.0%

Using Origin software, the sample curves were plotted and fitted by Gaussian function approximation. Gaussian fitting has the feature of fast and accurate calculation, so it was used for the analysis of the experimental data. [28] The changing trends were obtained as shown in Fig. 3, Fig. 4 and Fig. 5.

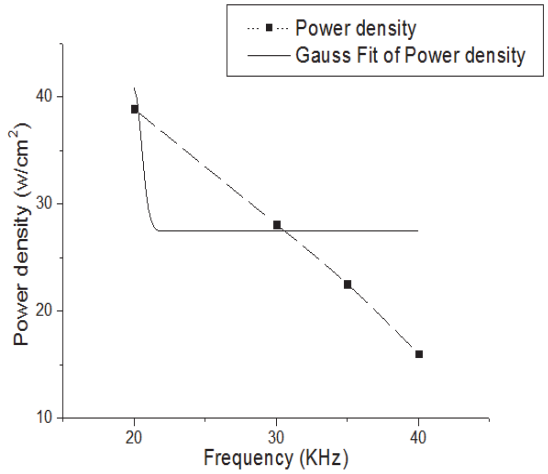

Figure 3 Ultrasonic ice drilling frequency sample strips and fitted curves (*I-f*)

4.1 Average Power Density

Average power density originated from the concept of thermal drilling, referring to the ratio of the system output power to the area of the tool head. It indicates the efficiency of input power and reflects the energy consumption rate of this drilling method. The above graph illustrates that in the range of 20~22 kHz, the average power density decreases linearly with the increase of frequency, and remains constant beyond 22 kHz. It indicates that with the increase of ultrasonic excitation frequency, using 22 kHz as the input frequency node, the input power of ultrasonic vibration system per unit area first decreases and then stabilizes, and the energy consumption during drilling gradually remains constant. It means that when the output frequency exceeds 22 kHz, the higher the vibration frequency, the more the energy consumption tends to be stabilized when the working condition allows. When the vibration output frequency is higher than 22 kHz, continuing to increase the vibration frequency will not increase too much energy consumption, which has guiding significance for selecting the optimal vibration frequency.

4.2 Drilling Speed

The Gaussian curve shown above has the same trend as the actual working curve, but there is some degree of delay. In terms of the degree of delay at the peak, the peak frequency of the Gaussian fitted curve is about 3 kHz higher than the actual curve. Combined with the actual situation and equipment on site, there are two reasons for this phenomenon. First, the ultrasonic generator is produced long ago, its variable amplitude rod and tool head design for a molding. With the using time increased, resonant frequency produces tiny errors, and its frequency is no longer precisely matched. Second, when starting the ultrasonic instrument, the piezoelectric ceramic transducer needs a certain amount of time to adjust the vibration field to adapt, and this frequency fluctuation caused by starting is inevitable. Therefore, the experimental results of the Gaussian curve are more in line with the ideal situation.

According to the Gaussian curve, the drilling speed gradually increases with the increase of frequency and then decreases, reaching the peak at 32 kHz, indicating that 32 kHz is the optimal excitation frequency for ultrasonic ice drilling in terms of drilling speed under the current experimental conditions. It may be related to the natural vibration frequency of the ice sample. When the applied ultrasonic frequency vibration reaches the range of the self vibration frequency of the ice sample, resonance occurs between the two, causing cracks to form in the ice sample. The cracks fuse and break into smaller fragments, thereby accelerating the melting speed.

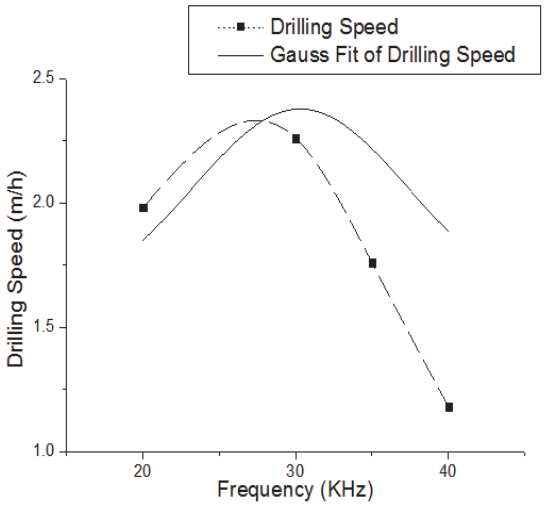

Figure 4 Ultrasonic ice drilling frequency sample strips and fitted curves (*η-f*)

4.3 Melting Rate

The melting rate is a more visual demonstration of the thermal effect from the heat conversion perspective. With the increase of frequency, the ice melting efficiency shows a trend of gradually increasing and then decreasing, and reached the maximum at 30 kHz, which means that 30 kHz was the optimal excitation frequency for ultrasonic ice drilling in terms of ice melting efficiency. Comparing Fig. 5 with Fig. 4, it can be seen that as the melting rate increases, the drilling speed also increases, indicating a positive correlation between the melting rate and the drilling speed. In Fig. 4, the ultrasonic vibration frequency corresponding to the peak drilling rate is 32 kHz. In Fig. 5, when the peak melting rate is reached, the applied ultrasonic vibration frequency is 30 kHz, which is 2 kHz earlier than the ultrasonic vibration frequency that reaches the highest drilling rate. Gaussian fitting curve from the graph above shows the effect of thermal energy conversion under ideal conditions. Therefore, this difference indicates that in ultrasonic vibration ice layer drilling, in addition to the method of melting the ice layer, mechanical vibration also assists in drilling to a certain extent.

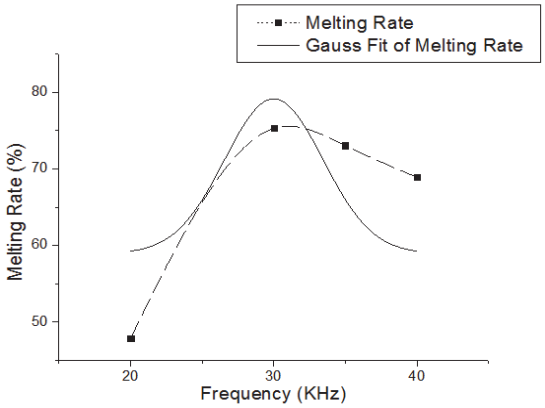

Figure 5 Ultrasonic ice drilling frequency sample strips and fitted curves (*V-f*)

5 CONCLUSIONS

Based on the experimental phenomena and summarizing the trends shown in the above three images, the main results of the current research are analyzed as follows.

1) From the observed experimental phenomena, it could be seen that the ice sample did not break up in large volume and there was water flowing out of the borehole under drilling pressure. Combining with the experimental phenomena and drilling mechanism analyzed, it is known that ultrasonic drilling is mainly characterized by melting ice, so the melting ice efficiency was taken as the main evaluation index and the calculation formula was deduced. The melting rate is positively correlated with the drilling speed, but there are differences between the two. A high melting rate indicates a high efficiency in thermal energy conversion. According to the experimental results, the ultrasonic vibration frequency corresponding to the peak drilling rate is delayed by 2 kHz compared to the ultrasonic vibration frequency applied when the peak melting rate is reached. This experimental phenomenon indicates that in ultrasonic vibration ice layer drilling, in addition to melting the ice layer, mechanical vibration also assists in drilling to a certain extent.

2) It is worth noting that ice in a solid state belongs to a hard brittle solid with a certain range of self vibration frequencies. There is a certain correlation between the mechanical crushing effect and the ultrasonic frequency. When the applied ultrasonic frequency vibration reaches the range of the self vibration frequency of the ice sample, the two resonate, causing cracks to form in the ice. The cracks fuse and split into smaller sized fragments. Moreover, due to the characteristic of the first melting point, small fragments melt faster.

3) The optimal value of ultrasonic ice drilling exists in the range of 30~32 kHz. In this range of frequency excitation, compared with the average power density, the drilling speed and ice melting efficiency of ultrasonic ice drilling were maximized, and the drilling was most economically efficient. The above experimental results were compared and analyzed with the data related to hot melt drilling. The conventional thermal melting drilling tool has a drilling speed of 2.18 m/h and an average thermal efficiency of 59% at an average power density of 25.85 $w \cdot cm^{-2}$. And the above experimental calculation results show that the drilling speed and thermal efficiency of ultrasonic ice melt drilling with a frequency of 30 kHz are 5% and 40.7% higher respectively, indicating that the ultrasonic drilling method is theoretically feasible and more efficient.

6 REFERENCES

[1] Tyler, S. W., Holland, D. M., Zagorodnov, V. et al. (2013). Instruments and Methods Using Distributed Temperature Sensors to Monitor an Antarctic Ice Shelf and Sub-ice-shelf cavity. *Journal of Glaciology*, *59*(215), 583-591. https://doi.org/10.3189/2013JoG12J207

[2] Thatje, S., Brown, A., & Hillenbrand, C. D. (2019). Prospects for Metazoan Life in Sub-glacial Antarctic lakes: The Most Extreme Life on Earth? *International Journal of Astrobiology*, *18*(5), 416-419. https://doi.org/10.1017/S1473550418000356

[3] Motoyama, H., Takahashi, A., Tanaka, Y. et al. (2020). The Second Deep Ice Coring Project at Dome Fuji, Antarctica. *Antarctic Record*, *64*, 284-329. https://doi.org/10.15094/00016228

[4] Cao, P., Yang, C., Chen, Y. et al. (2015). Experimental study of the drilling process in debris- rich ice. *Cold Regions Science and Technology*, *120*, 138-144. https://doi.org/10.1016/j.coldregions.2015.10.001

[5] Ekaykin, A. A., Bolshunov, A. V., Lipenkov, V. Y. et al. (2021). First glaciological investigations at Ridge B, central East Antarctica. *Antarctic Science*, *33*(4), 418-427. https://doi.org/10.1017/S0954102021000171

[6] Kim, H., Lee, J.W. (2002). Effect of ultrasonic wave on the degradation of polypropylene melt and morphology of its blend with polystyrene. *Polymer*, *43*(8), 2585-2589. https://doi.org/10.1016/S0032-3861(02)00017-4

[7] Palacios, J. L., Zhu, Y., Smith, E. C. et al. (2006). Ultrasonic shear and lamb wave interface stress for helicopter rotor de-icing purposes. *Collection of Technical Papers - AIAA/ASME/ASCE/AHS/ASC Structures, Structural Dynamics and Materials Conference*, *11*, 8131-8142.

[8] Hozumi, T., Saito, A., Okawa, S. et al. (2002). Freezing phenomena of supercooled water under impacts of ultrasonic waves. *International Journal of Refrigeration*, *25*(7), 948-953. https://doi.org/10.1016/S0140-7007(01)00104-9

[9] Marcelić, M. B., Geršak, J., Rogale, D. et al. (2022). Study of the compression properties of welded seams formed using hot wedge, hot air, ultrasonic, and high-frequency welding techniques. *Textile Research Journal*, *92*(23-24), 4736-4752. https://doi.org/10.1177/00405175221109637
[10] Hickling, R. (1965). Nucleation of Freezing by Cavity Collapse and its Relation to Cavitation Damage. *Nature*, *206*(4987), 915-917. https://doi.org/10.1115/1.3645809
[11] Kiani, H., Zhang, Z., Delgado, A. et al. (2011). Ultrasound assisted nucleation of some liquid and solid model foods during freezing. *Food Research International*, *44*(9), 2915-2921. https://doi.org/10.1016/j.foodres.2011.06.051
[12] Li, Y., Dong, X., Guo, W. et al. (2022). Ultrasonic micro-vibration deicing of flat plate for wind turbine blades. *Journal of Drainage and Irrigation Machinery Engineering*, *40*(2), 204-210. https://doi.org/10.3969/j.issn.1674-8530.20.0266
[13] Hayat, T., Inayatullah, Khan, S. A. et al. (2022). Significance of melting heat transfer in bio-convective thixotropic nanofluid. *Ain Shams Engineering Journal*, *13*(3), No.101625. https://doi.org/10.1016/j.asej.2021.10.020
[14] Chatterjee, D., Chaitanya, N. V. V. K., & Mondal, B. (2022). Analysis of the thermo-fluidic transport around counter-rotating tandem circular cylinders. *Proceedings of the Institution of Mechanical Engineers, Part C: Journal of Mechanical Engineering Science*, *236*(7), 3418-3433. https://doi.org/10.1177/09544062211042043
[15] Li, L., Li, H., Kou, G. et al. (2022). Dynamic Camouflage Characteristics of a Thermal Infrared Film Inspired by Honeycomb Structure. *Journal of Bionic Engineering*, *19*(2), 458-470. https://doi.org/10.1007/s42235-021-00141-5
[16] Zhao, K., Wu, J., Li, X. et al. (2021). Advances of Ultrasonic Scaling Removal Technology and Heat Transfer Enhancement Technology. *ChemBioEng Reviews*, *8*(2), 134-144. https://doi.org/10.1002/cben.202000020
[17] Yin, S., Zhao, D., & Zhai, G. (2016). Investigation into the characteristics of rock damage caused by ultrasonic vibration. I*nternational Journal of Rock Mechanics and Mining Sciences*, *84*, 159-164. https://doi.org/10.1016/j.ijrmms.2015.12.020
[18] Wang, S., Zhang, J., Li, C. et al. (2022). Seepage characteristics of fractured rock mass with non-equal width filling under cyclic loading. *Ain Shams Engineering Journal*, *13*(6), 101794. https://doi.org/10.1016/j.asej.2022.101794
[19] Wiercigroch, M., Wojewoda, J., & Krivtsov, A. M. (2005). Dynamics of ultrasonic percussive drilling of hard rocks. *Journal of Sound and Vibration*, *280*(3-5), 739-757. https://doi.org/10.1016/j.jsv.2003.12.045
[20] Aganin, A. A. & Davletshin, A. I. (2019). Interaction of Cavitation Bubbles in Acetone at Their Strong Enlargement and Collapse. *Lobachevskii Journal of Mathematics*, *40*(6), 699-704. https://doi.org/10.1134/S1995080219060027
[21] Maisonhaute, E., Brookes, B. A., & Compton, R. G. (2002). Surface acoustic cavitation understood via nanosecond electrochemistry. 2. The motion of acoustic bubbles. *Journal of Physical Chemistry B*, *106*(12), 3166-3172. https://doi.org/10.1021/jp013448a
[22] Maisonhaute, E., Prado, C., White, P. C. et al. (2002). Surface acoustic cavitation understood via nanosecond electrochemistry. Part III: Shear stress in ultrasonic cleaning. *Ultrasonics Sonochemistry*, *9*(6), 297-303. https://doi.org/10.1016/S1350-4177(02)00089-5
[23] Ahmad, I., Faisal, M., Javed, T. et al. (2022). Insight into the relationship between unsteady Cattaneo-Christov double diffusion, random motion and thermo-migration of tiny particles. *Ain Shams Engineering Journal*, *13*(1), No.101494. https://doi.org/10.1016/j.asej.2021.05.008
[24] Brujan, E. A. (1999). A first-order model for bubble dynamics in a compressible viscoelastic liquid. *Journal of Non-Newtonian Fluid Mechanics*, *84*(1) 83-103. https://doi.org/10.1016/S0377-0257(98)00144-X
[25] Kontek, M., Strojin, S., Clifton Brown, J. et al. (2022). Combustion Calorimetry as a New Method of Composition and Heating Value Determination of Miscanthus - An Early View. *Tehnicki Vjesnik*, *29*(5), 1721-1725. https://doi.org/10.17559/TV-20210708101840
[26] Ratcliffe, E. H. (1962). The thermal conductivity of ice new data on the temperature coefficient. *Philosophical Magazine*, 7(79), 1197-1203. https://doi.org/10.1080/14786436208209120
[27] Benfield, A. E. (1940). Thermal measurements and their bearing on crustal problems. *Eos Transactions American Geophysical Union*, *21*(2), 155-159. https://doi.org/10.1029/TR021i002p00155
[28] Agarski, B., Sokac, M., Santosi, Z. et al. (2020). Multi-criteria evaluation of design complexity for patient-specific bone graft. *Tehnicki Vjesnik*, *27*(3), 803-811. https://doi.org/10.17559/TV-20190605103211

Contact information:

Chen WANG, Candidate for PhD
College of Construction Engineering, Jilin University
130026, Changchun, Jilin, China

DaJun ZHAO, Doctoral Supervisor
(Corresponding author)
College of Construction Engineering, Jilin University
130026, Changchun, Jilin, China
E-mail: cw19@mails.jlu.edu.cn

Xin FANG, University Lecturer
Jilin University of Construction, School of Civil Engineering
130118, Changchun, Jilin, China